sciendo Applied Mathematics and Nonlinear Sciences, 9(1) (2024) 1-16

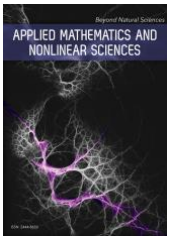

Applied Mathematics and Nonlinear Sciences

https://www.sciendo.com

The Use of AI Technology in Digital Ceramic Technology

Huayan Zheng[1,†], Yaqian Hu[1], Jing Yang[1]

1. Jiangxi Arts &Ceramics Technology Institute, Jingdezhen, Jiangxi, 333000, China.

Submission Info

Communicated by Z. Sabir
Received March 18, 2024
Accepted June 6, 2024
Available online July 2, 2024

Abstract

With the development of AI technology, the development of the ceramic industry has ushered in a good opportunity. This paper discusses the application of AI technology in the field of ceramics on the basis of deep convolutional generative adversarial network, using Adam optimizer to further improve the performance of the model, using the hidden space to add noise to each layer of the network, and proposing a digital ceramic texture image generation model based on DCGAN. Meanwhile, the K-Means algorithm and feature fusion mechanism with BWP as the evaluation index are introduced to improve the Faster R-CNN algorithm and construct the ceramic defect detection model. The scores of each subjective evaluation index of image generation quality are greater than 4, which are located in the interval of higher evaluation. The scores of IS, BRISQUE, and NIQE are 3.39, 22.57, and 4.43, and the quality of ceramic texture image generation of this paper's model is better than that of other algorithms. The ceramic defect detection model's detection accuracy for all five ceramic defects is higher than 92.68%, with an 8.54% improvement over the original algorithm's defect detection performance. The research in this paper has important theoretical and practical significance for ceramic product design, quality control, and troubleshooting of production equipment.

Keywords: DCGAN; Faster R-CNN; Image generation; Defect detection; Digital ceramics.
AMS 2010 codes: 97P10

†Corresponding author.
Email address: 13879833320@163.com

ISSN 2444-8656
https://doi.org/10.2478/amns-2024-1503

sciendo
OPEN ACCESS © 2023 Huayan Zheng, Yaqian Hu and Jing Yang, published by Sciendo.

CC BY This work is licensed under the Creative Commons Attribution alone 4.0 License.

1 Introduction

Ceramic art, as an ancient and rich art form, has been continuously developing and evolving [1]. And with the rapid development of digital technology, ceramic art has gradually intersected with digital technology. Digital technology provides ceramic artists with new creative tools and forms of expression and also changes the ceramic manufacturing process and the display of ceramic works [2]. Digital technology has brought more innovative tools and forms of expression for ceramic art and, at the same time, changed the ceramic manufacturing process and the way of displaying ceramic works [3].

The application of digital technology provides more space for innovation and development of ceramic art. However, it also brings some challenges [4]. Therefore, ceramic artists need to flexibly use digital technology while preserving traditional craftsmanship in order to achieve a balance between creation and innovation. In the future, the intersection of digital technology and ceramic art will continue to promote the development of ceramic art and bring more possibilities and experiences to ceramic artists and audiences [5-6].

The development of the ceramic industry is also inseparable from the implantation of new artificial intelligence technology. Its positive effects are mainly manifested in the optimal use of ceramic materials, the improvement and enhancement of product performance, the monitoring and management of the production process, the market development of product marketing, etc. [7-8]. The use of new artificial intelligence technology is also more extensive, which has made an important contribution to the revitalization of China's ceramic industry economy and improved the productivity level of the ceramic industry. Of course, artificial intelligence is not omnipotent. Although it has achieved great success in many areas, but still faces some bottlenecks in the application. From the theory, artificial intelligence can be interpreted poorly, ethical alignment difficulties, cognitive reasoning ability is weak in the practical application, data acquisition difficulties, the lack of core technology, the talent team is weak, the scale of the enterprise and the implementation of artificial intelligence does not match, and so on. These problems in the development of the issues that we must face, of course, these problems will ultimately be in the new generation of artificial intelligence itself to upgrade and ceramic industry to comply with the latest technological changes in the advancement of the gradual breakthrough [9-10].

Artificial intelligence, a new technology using imitation of human brain intelligence, to achieve super artificial performance, is widely used in various industries. The ceramic industry, because it introduced new artificial intelligence technology, product optimization, production intelligence monitoring, and marketing of all aspects, has produced unprecedented changes. Artificial intelligence technology has effectively enhanced the market competitiveness of ceramic products and enterprise efficiency and become a typical case of China's manufacturing industry from traditional to modern transformation. We discuss this phenomenon and its future development trend, hoping to form a consensus on the theory and better promote the new revitalization of the ceramic industry. Yu, G. et al. used digital image technology to investigate the shear performance of ceramic composite z-pin and the factors affecting it. Based on the experimental results, it was learned that the improvement of the structure of the plain weave pin and the related parameters is an effective way to improve the composite material's resistance to shear [11]. Chen, et al. developed and fabricated a Si3N4-SiO2 composite ceramic using digital light processing 3D printing technology, which has good wave transparency performance [12]. A, Y. Z. et al. prepared a zirconia (ZrO2) ceramic dental implant abutment based on the DLP3D printing technology and examined the anisotropic properties of the ceramic of this material. The test results showed that the smaller the pre-turn angle of the sample, the more safe the ZrO2 ceramic was. The smaller the pre-turn angle of the sample, the higher the safety factor [13]. Tang, D. et al. introduced degreasing and sintering procedures to ceramic slurry for

processing to prevent the problem of surface defects in ceramic preparation and combined with the DPL technique for the Al_2O_3/SiO_2 ceramics and experimentally corroborated the electromagnetic shielding capability of the TPMS structure [14]. Zhang, S. et al. conceptualized a ceramic additive manufacturing (AM) strategy to overcome the problem of shape-structure defects in the ceramic raw material ilmenite and effectively strengthened the printing properties of ilmenite [15]. Furushima R. et al. built an analytical framework based on a convolutional neural network algorithm to evaluate the fracture toughness and flexural properties of silicon nitride ceramics, and the results of the study provide an important reference for the application and performance optimization of silicon nitride ceramics [16]. Mu, X. L. H et al. introduced AI technology into ancient ceramics appraisal, which can be used to appraise ceramic appraisal in more complex situations. In practice, the ceramic identification method based on AI technology achieves a certain degree of accuracy and can be competent in the identification of ancient ceramics [17]. He, Y. emphasized the positive role played by AI technology and data mining technology in the design of ceramic products, which promotes the designers to develop ceramic product design thinking and promotes the innovation of ceramic products [18]. Tian, Y. et al. tried to combine the SWOT analysis method to dig deeper into the development of China's ceramic industry and think about how to apply computer technology to achieve the design and preparation of Chinese ceramic colors and materials. The research has a positive reference significance for the development and upgrading of China's ceramic industry [19].

The focus of this study is on ceramic defect detection techniques that are supported by artificial intelligence technology. The study takes DCGAN implemented by the convolutional network as a prototype, uses Adam optimizer as a new optimizer for the network, introduces Gaussian noise to improve the hidden space, and constructs a ceramic texture image generation model. In addition, the Faster R-CNN algorithm is improved. The K-Means algorithm based on the BWP metric is used to generate an initial bounding box suitable for generating morphological features of the image ceramic surface imperfections. The feature maps with different resolutions are united to construct a more sensitive ceramic imperfection detection model. On this basis, the quality of the images generated by this algorithm is detected using five indicators: average image generation time, maximum image resolution, IS, BRISQUE, and NIQE. By detecting five different types of ceramic defects and comparing the detection effect of other algorithms, we verify the performance of the improved Faster R-CNN model for detecting ceramic defects. Explore the strategy of AI technology to empower the development of the digital ceramic industry.

2 DCGAN-based digital ceramic texture image generation

2.1 Deep Convolutional Generative Adversarial Network Modeling

By adding noise, ceramic texture image generation can create false images that are indistinguishable from the naked eye. Primitive GANs and CGANs mostly use multi-layer feed-forward neural networks for image generation. Training GANs are unstable, and unsupervised learning usually results in meaningless outputs from the generator. Deep Convolutional Generative Adversarial Network (DCGAN) uses a convolutional neural network to construct the generator and discriminator in the GAN. It adjusts the structure, activation function, and training method of the convolutional neural network in order to improve the quality of the generated ceramic texture images, accelerate the training speed of the model, and enhance the stability of the network.

The contributions made by DCGAN include fully convolutional networks, removal of fully connected layers, bulk normalization (BN), use of ReLU activation function, and LeakyReLU activation function.

2.1.1 Batch normalization (BN)

The training process of the deep neural network may encounter the phenomenon of internal covariate leveling, which can be resolved by adding a normalization layer. After the normalization of the batch process, the initialization of the model does not need to be overly concerned about the choice of the learning rate. The initial learning rate of the model can also be preset to a higher value, while in some cases, the model can also be replaced for the use of Dropout.

Suppose a layer in the middle of the network gets features distributed on both sides of the Sigmoid function by forced normalization. In that case, the normalization operation controls the standard deviation of the feature data to 1 and transforms the data into the linear part of the activation function. This results in the distribution of features learned from this level of extraction being modified and corrupted, leading to a learning failure. Therefore, two parameters are added γ, β with variable parameters to control the weighting. The formula is as follows:

$$y^{(k)} = \Upsilon^{(k)} \hat{x}^{(k)} + \beta^{(k)} \tag{1}$$

In this way each neuron has its specific pair of parameters. The formula for its forward conduction process:

$$\mu_B \leftarrow \frac{1}{m} \sum_{i=1}^{m} x_i \tag{2}$$

$$\sigma_B^2 \leftarrow \frac{1}{m} \sum_{i=1}^{m} \left(x_i - \mu_B \right)^2 \tag{3}$$

$$\hat{x}_i \leftarrow \frac{x_i - \mu_B}{\sqrt{\sigma_B^2 + \varepsilon}} \tag{4}$$

$$y_i \leftarrow \Upsilon \hat{x}_i + \beta \equiv BN_{\Upsilon,\beta}\left(x_i \right) \tag{5}$$

2.1.2 Adam Optimizer

The task of machine learning is to optimize the parameters of each layer to their most suitable values, i.e., to minimize the time loss function. The loss function is a function of the difference between the value of the objective function and the actual value, which is actually a function of the optimized parameters. The task of the optimizer is to calculate the gradient of the loss function for each epoch and then update the parameters. In the experiments in this chapter, the network model is optimized using the Adam optimizer for the generator and the discriminator.

The method is based on the first and second-order derivatives of the gradient for estimating the individual adaptive learning rate for different parameters. But, for a set of input training samples x and its label y, the model based on multiple inputs x through the parameter calculation to get the predicted value of the sample y', and the original label value of the sample for the difference between the calculation that is to calculate the loss function of the model, and the results will be used as the optimizer's objective function. This objective function is used to find the gradient (some optimizers also require momentum). Then, the parameters are updated using the gradient value (momentum) until the stopping condition is reached.

The specific way the Adam optimizer updates its parameters is as follows:

First, the gradient of the time step is computed:

$$g_t = \nabla_\theta J\left(\theta_{t-1}\right) \tag{6}$$

Next, calculate the part of the momentum gradient that is decreasing:

$$m_t = \beta_1 m_{t-1} + \left(1-\beta_1\right) g_t \tag{7}$$

$$v_t = \beta_2 v_{t-1} + \left(1-\beta_2\right) g_t^{\,2} \tag{8}$$

The gradient mean and gradient squared mean are then bias-corrected:

$$\hat{m}_t = m_t \Big/ \left(1-\beta_1^t\right) \tag{9}$$

$$\hat{v}_t = v_t \Big/ \left(1-\beta_2'\right) \tag{10}$$

Finally, update the parameters:

$$\theta_t = \theta_{t-1} - \alpha * \hat{m}_t / \left(\sqrt{\hat{v}_t} + \varepsilon\right) \tag{11}$$

2.1.3 Hidden Space Improvement Algorithm

Due to the excellent performance of Deep Convolutional Generative Adversarial Networks (DCGAN) in generating ceramic texture images, this paper uses the method of increasing hidden space vectors to train the model on this basis. The quality of ceramic texture-generated images is directly affected by the secret space vector. Therefore, the random noise vector z is input to each feature extraction layer of the generator G, instead of the traditional method of linking only the original ceramic images as the training input for the model. This approach allows the generator to use the "hidden space", i.e., A feature space of the input noise that can directly influence features in different resolutions and layers. The hidden layer allows each layer to receive the hidden space vectors, i.e., The noise, along with the ceramic image vectors inputted from the previous layer. This chapter utilizes Gaussian noise as an additive noise. This is done by dividing the noise vector z into a block for each resolution and then connecting it to the condition vector c mapped to each layer. This allows the implicit vector space to be used to directly affect the features at different resolutions as well as at various levels. The addition of noise is randomized to avoid the same features being extracted each time due to the addition of the same noise. Although some memory space will be sacrificed with the addition of noise, the accuracy of the model and the training speed of this method will continue to improve with the increase in the number of iterations.

2.2 Experimental results and analysis

This section conducts a series of experiments to verify the effectiveness of the proposed algorithm in this chapter. Firstly, grayscale texture images and style sample data sets are produced based on large ceramic photos and other images from a well-known company, and the experimental environment is

set up simultaneously. The algorithms in this chapter and other algorithms produce ceramic texture images, and the quality of the image is comprehensively analyzed and compared through qualitative and quantitative forms. The experimental process and results are described in turn.

2.2.1 Data set construction

Gray scale texture image dataset construction: 40 large ceramic images are selected in this chapter, with image sizes larger than 4096px×4096px. For each large ceramic image, about 60 texture images of 256px×256px are randomly cropped. Then, among all the texture images, those with higher texture complexity are selected for grayscaling. The final selected 2000 grayscale texture images will constitute the dataset for training the Adam-DCGAN network.

Construction of stylistic samples: In this chapter, 15 images with higher resolution and more distinctive stylistic features are selected simultaneously. The production of ceramics is partly based on natural texture maps and part on oil and watercolor paintings that are suitable for ceramic production. The Adam-DCGAN network will be trained on each sample image of each style, and the trained model will be added to the style pool for ceramic image generation style selection.

2.2.2 Ceramic Texture Image Generation Results and Analysis

1) Evaluation of the quality of generated images

A set of questionnaires is used to evaluate the subjective quality of images generated by different algorithms in this subsection. When comparing algorithms, the same input data is used, and each algorithm is compared with 10 randomly generated image sets. Then, 60 people were randomly invited to score the respective image quality evaluation factors of the image set, and the average was taken as the final result. The image quality evaluation factors involved in the questionnaire are (1) image diversity, (2) degree of preservation of major texture features, (3) style migration effect, (4) image size, and (5) image quality. All the image quality evaluation factors were rated in the range of 0 to 5, and a rating range falling in the interval [0,1.5] is a low degree of the evaluation factor, (1.5,3] is a medium degree, and (3,5] is a high degree.

The results of image quality evaluation of different algorithms are shown in Table 1. Although the algorithms based on image editing have better preservation of image texture features, with scores of 3.02 and 3.43 for the degree of major texture preservation, which is a high evaluation scale, they lack diversity due to the small number of missing parts of the image, i.e., Editing the missing parts of the image based on a large number of a priori features, and still need to be improved in terms of size and quality of the image. In the AutoEncoder/GAN-based algorithms, the image diversity scores are all located in the interval of 3 to 5. The degree of preservation of the main texture is greater than 1.5, which is able to increase the diversity of the output image by changing the input vectors and has a more obvious texture characteristic. Still, these algorithms are unable to control the stylistic characteristics of the output ceramic texture image to achieve the selection of a specific style. In the algorithm based on style migration, although the output ceramic texture image diversity can be increased by changing the input style image, compared with the algorithms in this chapter due to the image size and quality degradation, the effect of image style migration is not ideal. It will cause degradation of the degree of retention of image texture. The algorithm in this paper scores more than 4 on image diversity, retention of major texture features, style migration effect, image size, and image quality, and its generated images are well evaluated on various features.

Table 1. Image quality evaluation results of different algorithms

Category	Algorithm name	Image Diversity	Key texture retention	Style migration effect	Image size	Image quality
Image editing	Pixel-CNN	1.69	3.02	—	0.54	0.74
	DIP	1.81	3.43	—	0.77	1.89
AutoEncoder /GAN network	UNet	3.39	1.75	—	2.22	0.94
	StyleGAN	3.54	1.81	—	2.58	1.13
	DCGAN	3.66	1.84	1.24	2.16	1.29
	GAN-Sketching	3.71	3.34	—	2.38	1.25
Style migration	Basic style migration	3.04	0.52	1.41	0.62	1.35
	MGANs	3.82	0.63	0.83	0.76	1.43
	Texture synthetic GAN	4.04	0.66	1.37	2.72	2.85
Algorithm of this article		4.12	4.08	4.49	4.81	4.05

2) Evaluation of quantitative results

This subsection introduces five indicators, namely, average image generation time, maximum image resolution, IS, BRISQUE, and NIQE, to further quantitatively compare the image quality evaluation factors. The evaluation of quantitative indicators involves image quality, diversity and other aspects to make the evaluation results more objective and comprehensive. Among them, IS is used to evaluate the diversity and authenticity of network-generated images, and the higher the score, the better the overall effect; BRISQUE and NIQE are used to assess the overall quality of generated images, and the lower the score, the stronger the image quality.

The ceramic texture image generation quality results are shown in Fig. 1. Where (a)~(d) is the average image generation time, and (e)~(h) are the maximum image resolution, IS, BRISQUE, and NIQE metrics results, respectively. The image generation time of this paper's model ceramic texture is 1.21s (256px), 3.01s (1024px), 35.7s (4096px), and 46.8s (16384px), which is slightly higher than other networks and algorithms in the average image generation time. Still, the maximum image resolution is greatly increased. The IS score of this algorithm is 3.39, which is higher than the rest of the style migration algorithms, further proving that the model in this paper is capable of generating more diverse and natural-looking ceramic texture images. In terms of BRISQUE and NIQE scores, the algorithm scores 22.57 and 4.43, which are lower than the other comparison algorithms, and the overall image quality is the best.

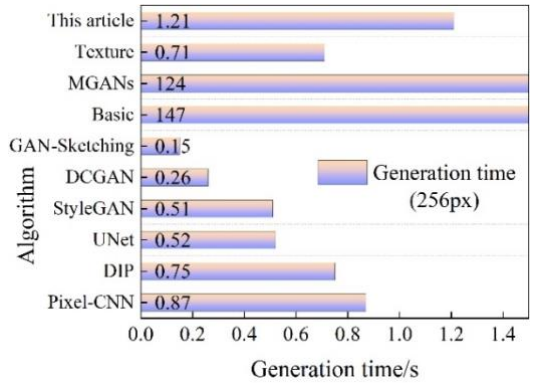

(a) Generation time (256px)

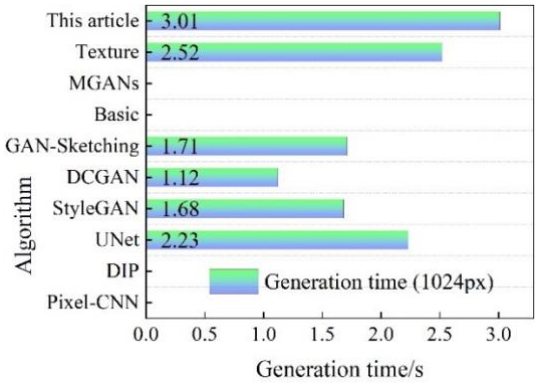

(b) Generation time (1024px)

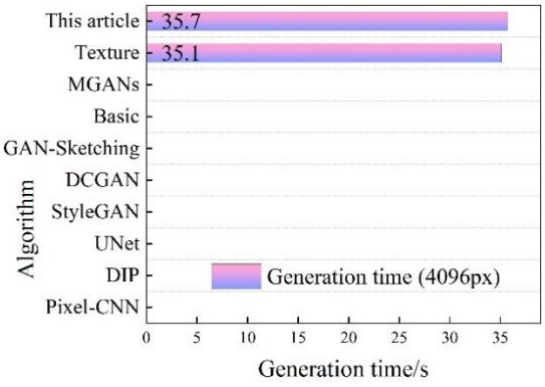

(c) Generation time (4096px)

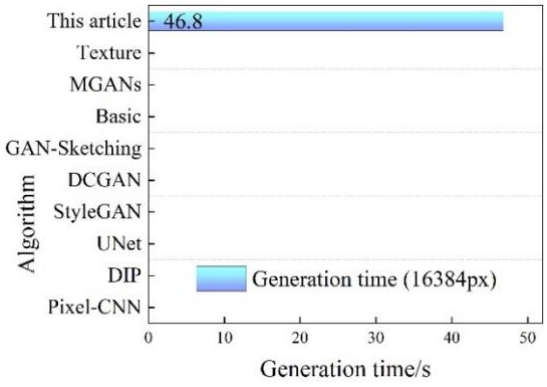

(d) Generation time (16384px)

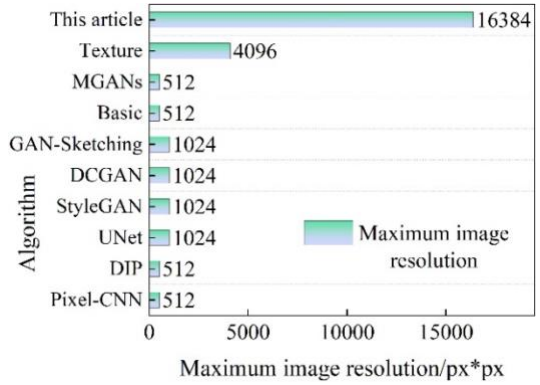

(e) Maximum image resolution

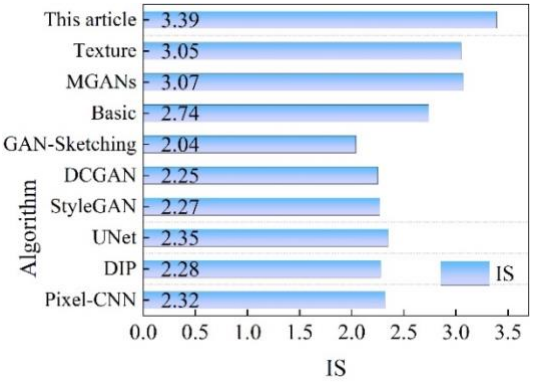

(f) IS

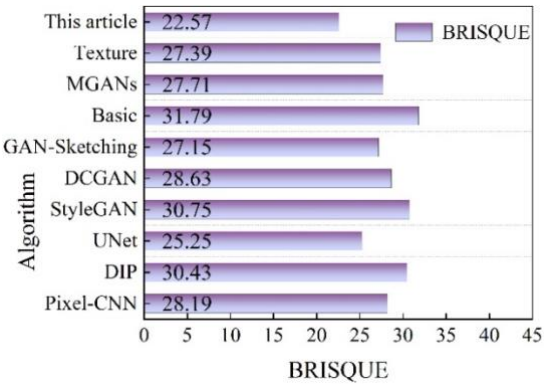

(g) BRISQUE

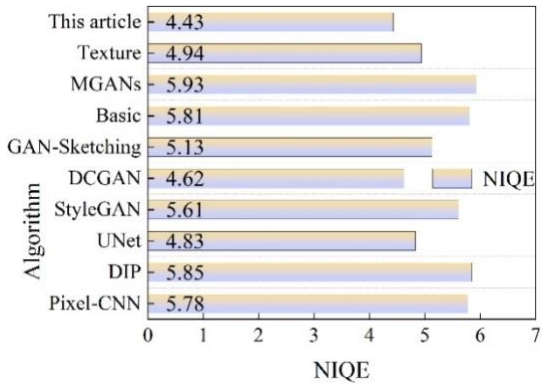

(h) NIQE

Figure 1. Ceramic texture image generates quality results

3 Ceramic Defect Detection Based on Improved Faster R-CNN

3.1 Improved Faster R-CNN Defect Detection Model

The Faster R-CNN model has a better detection effect on ceramic surface defects, and this chapter makes two main improvements to Faster R-CNN. First, the K-Means algorithm based on BWP metrics is used to generate an initial bounding box suitable for the morphological features of ceramic surface defects. Secondly, feature maps with different resolutions are combined to ensure that the

final feature matrix generated by the model is equally sensitive to micro-defects. Through the above improvement methods, the model's ability to detect micro-defects as well as morphologically similar defects has been improved.

3.1.1 Feature extraction network

The structure of Faster R-CNN is shown in Fig. 2. The final detection results are greatly influenced by the feature extraction layer, which is one of the most important components of the network. We will be introducing the feature extraction network VGG16 in the Faster R-CNN framework and examining how the size of the feature map sensory field affects target detection.

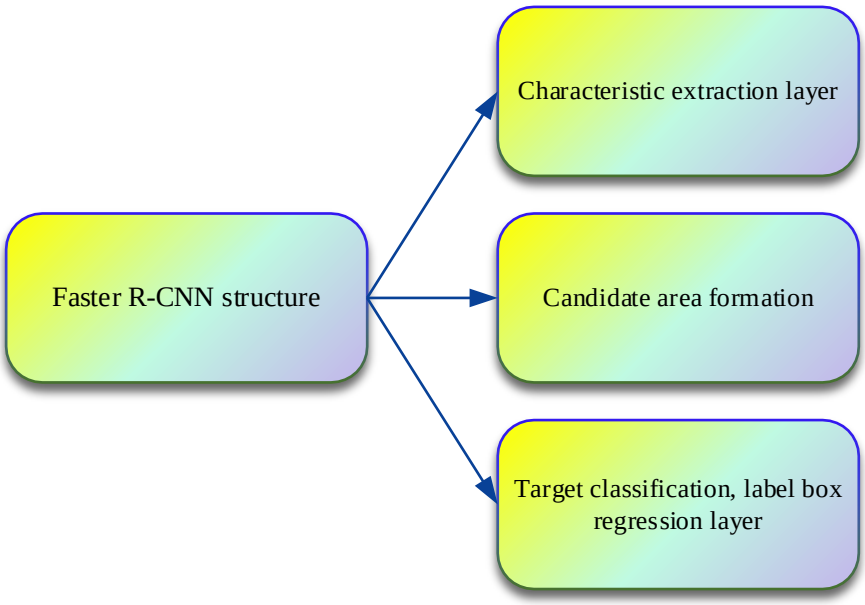

Figure 2. Faster R-CNN structure

In the VGG16 network, the convolution kernels are all of size 3*3, the convolution step is 1*1, the pooling layer uses maximum pooling, and the feature matrix is integrated using fully connected layers. 16 layers are both convolutional and fully connected. The receptive field is the region where a point on the feature matrix is mapped onto the training sample after passing through the layers.

The size of the neuron's receptive field is only affected by the convolution kernel as well as the convolution step size, which is calculated as shown in equation (12):

$$l_k = l_{k-1} + \left[\left(f_k - 1 \right) * \prod_{i=1}^{k-1} s_i \right] \tag{12}$$

Where l_k denotes the current layer receptive field, l_{k-l} denotes the previous layer receptive field, the size of the current layer convolutional kernel is denoted as f_k, the convolutional step size is denoted as s_i, and the size of the receptive field is proportional to the degree of abstraction of the image features.

3.1.2 Candidate frame size clustering

Since the defective region accounts for too small a proportion of the background region, and defects of the same type may have multiple morphologies, directly using the original Faster R-CNN corresponding to the Anchor box can not effectively frame the defective region. Therefore, the length and width of the defect labeling box in Ground Truth are used as the coordinate points. The clustering algorithm is introduced to generate the initial labeling box suitable for the defects on the ceramic surface. The length and width ratios obtained by clustering are used to replace the parameters corresponding to the original anchor points in Faster R-CNN.

K-Means uses Euclidean distance as the classification criterion and divides the data into K class by unsupervised learning, and the distance from each class to the center point of the current subclass is sufficiently small, i.e., The center point of each cluster has great representativeness, which is in line with the requirements of this paper for defective clustering. The data involved in clustering is divided into K classes, then the classification criterion is shown in equation (13):

$$\min J_W\left(C_1,\ldots,C_K\right)=\frac{1}{n}\sum_{j=1}^{K}\sum_{x\in C_j}\left\|x-m_j\right\|^2, m_j=\frac{1}{n_j}\sum_{x\in C_j}x \tag{13}$$

Where C denotes the subclass of clustering, n is the number of samples to be clustered, K denotes the number of categories generated after the algorithm is run, m is the centroid of the newly generated subclass, and x denotes the dimensions of the outer rectangle of the ceramic surface defects in Groundtruth.

Certain different types of ceramic surface defects usually have similar external contours, so the initial labeled boxes generated not only need sufficient intra-class distances but also inter-class distances should be maximized as well. The clustering number K of K-Means is determined manually, and the algorithm only considers the intra-class distance but ignores the important inter-class distance, thus leading to poor clustering accuracy and unsatisfactory results. In order to comprehensively consider the classification criteria of the labeled boxes, this paper uses BWP as the clustering evaluation index to determine the optimal number of clustering centers k_{out}, so that the clustered samples have sufficient differentiation, i.e., small intraclass differences and large interclass differences. The calculation method of k_{out} is shown in equation (14):

$$k_{out}=\max\{avgBWP(k),k\in[2,)\} \tag{14}$$

The K-Means algorithm based on the BWP indicator selects the number of cluster centroids k sequentially within $[2,n)$, so that the evaluation indicator $avgBWP(k)$ takes the maximum value of k that is the number of cluster centroids. The calculation method of $avgBWP(k)$ is shown in equation (15):

$$avgBWP(k)=\frac{1}{n}\sum_{j=1}^{k}\sum_{i=1}^{n_j}BWP(j,i) \tag{15}$$

The above equation, $BWP(j,i)$ assesses both the degree of discrete as well as the degree of intra-class closeness of each subcategory, which is calculated as shown in equation (16). j is the category label, i is the sample subscript, and $BWP(j,i)$ denotes the BWP metric for the ith sample in j categories:

$$BWP(j,i)=\frac{b(j,i)-w(j,i)}{b(j,i)+w(j,i)} \tag{16}$$

The above equation, $b(j,i)$ denotes the average distance of the ird sample in category j to the closest of the rest of the category, which is used to measure the degree of dispersion between the different categories, as shown in equation (17). $w(j,i)$ denotes the average distance of the ith sample in category j to the rest of the samples in this category, which is used to measure the closeness of the category, as shown in equation (18):

$$b(j,i)=\min\left(\frac{1}{n_m}\sum_{b=1}^{n_m}\left\|x_b^{(m)}-x_i^{(j)}\right\|^2\right),1\le m\le k,m\ne j \tag{17}$$

Where, j,m denotes the different categories, i denotes the number of the sample, n_m denotes the number of samples in category m. $x_i^{(j)}$ denotes the ith sample of category j, and $x_b^{(m)}$ denotes the bth sample of category m. $\|\square\|^2$ denotes the square of the distance between the two sample points involved in the calculation. After the above calculation, the nearest category to $x_i^{(j)}$ is obtained.

$$w(j,i)=\frac{1}{n_j-1}\sum_{q=1,q\ne i}^{n_j}\left\|x_q^{(j)}-x_i^{(j)}\right\|^2,j=1,2,\ldots,k \tag{18}$$

The above equation, n_j denotes the number of sample points included in class j, and $x_q^{(j)}$ denotes the sample point subscripted as q in class j.

3.1.3 Multi-scale feature map fusion

The research object of this chapter is the defects, such as cracks and pinholes on ceramic surfaces, and the purpose of the research is to recognize the type of defects and label the location of the defects. However, the above defects account for too small a proportion of the image, the area is too random, and some different types of defects often have similar morphological features. If the standard Faster R-CNN model is used directly to train and detect, the phenomenon of inaccurate localization and missed detection will occur. In order to solve this problem, this paper combines the last two layers of feature maps on the basis of the standard VGG16 network, which is used as the input for subsequent defect classification and coordinate regression.

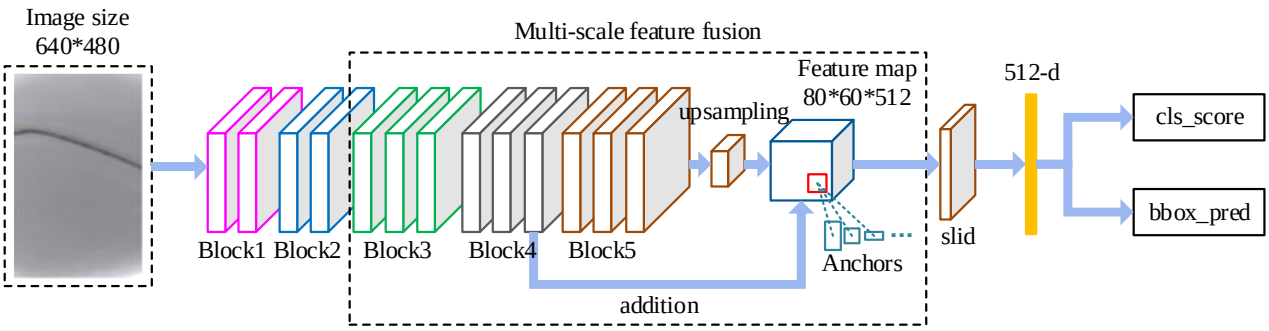

Figure 3. Feature extraction network

The improved feature extraction network's structure is depicted in Fig. 3, and the final output feature map of the model is combined with the feature matrices of the last two blocks. The model first expands the dimension of the feature map output from the previous block and then fuses the feature with the production of the feature from block 4. By using a fused feature map, the model can detect defects with small dimensions or similar morphology.

3.2 Experiments and analysis of results

Ceramic images with defects are collected as a dataset for defect labeling, and a total of 10,000 training samples are clipped on the dataset to identify and localize the surface defects of ceramics using the improved Faster R-CNN model.

3.2.1 Model training

In this paper, the confidence loss function of the original Faster R-CNN model is first used to train 100 rounds (Epoch) until the model is stabilized. Then, the confidence loss function of the improved Faster R-CNN model is used to continue training for 100 Epoch.

The total training Epoch for this experiment is 200, the Batch size is 4, and the initial learning rate is 0.001, which decays to 0.0001 after the 50th Epoch. The loss value curve of the ceramic defect detection model is shown in Fig. 4, and the loss value tends to stabilize when the Epoch reaches 200 times and finally stabilizes at about 13.53.

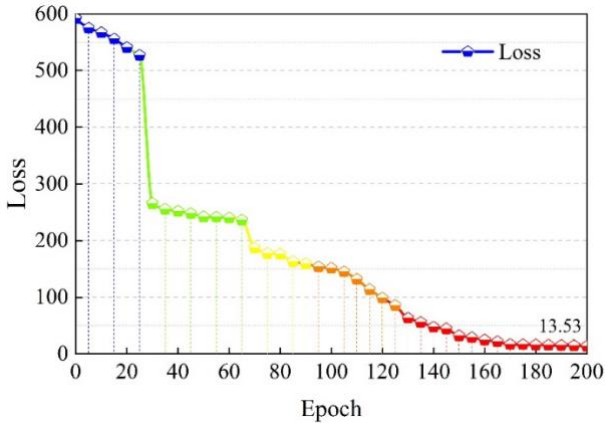

Figure 4. The loss value curve of the ceramic defect detection model

3.2.2 Effectiveness of Ceramic Defect Detection

The number of pictures to be detected is 200. Each image contains 1 to 5 categories of defects (stains, foreign objects, multi-gold, damage, lack of porcelain). Ceramic defect detection results are shown in Table 2, where the accuracy rate indicates the proportion of correctly predicted positive samples of defects to the proportion of positive samples of defects in all the prediction results, and the recall rate indicates the proportion of correctly predicted positive samples of defects to the proportion of positive samples of all the actual defects.

The improved Faster R-CNN model in this paper achieves a detection accuracy and recall rate of more than 92.68% and 95.35% for five different kinds of defects in ceramics, namely, stains, foreign objects, multi-gold, damage, and lack of ceramics, which basically meets the requirements needed for the actual production of this task.

Table 2. Ceramic flaw detection results

Defective category	Total amount	Correct detection	Mis check	Leak detection	Accuracy / %	Recall rate / %
Stain	1045	1021	11	24	98.92%	97.70%
Foreign matter	37	37	0	0	100.00%	100.00%
Dorkin	43	41	3	2	92.68%	95.35%
Lesion	358	346	15	12	95.66%	96.65%
Deficient porcelain	95	91	4	4	95.60%	95.79%
Total	1578	1536	33	42	97.85%	97.34%

In order to further verify the effectiveness of the improved Faster R-CNN model in this paper on ceramic defect detection, the algorithm of this paper is compared with the common target detection algorithms Faster R-CNN, Efficientdet-D3, YOLOv5, YOLOX, and YOLOv4 for a comparison test on this paper's dataset. The experimental parameters of the original authors are used, and the following are selected: average accuracy, average recall, and detection time per image as evaluation metrics.

The performance of different algorithms for ceramic defect detection is shown in Table 3. The improved Faster R-CNN model in this paper achieves an average accuracy and recall of 91.72% and 92.56% for ceramic defect detection, which is 8.54% and 8.23% higher than the original Faster R-CNN algorithm, respectively. Faster R-CNN is not effective in this task due to its poorer performance in small target detection. Although Efficientdet-B3 has a better balance between real-time and detection performance, it still does not perform well in this task. Although other algorithms also achieve good detection results, and in the detection of real-time better than the proposed ceramic defect detection algorithm, taking into account the average accuracy and the average recall rate, and according to the requirements of the detection speed, the proposed ceramic defect detection algorithm can complete the detection of each picture in 0.197s, which basically meets the requirements of the industrial field detection.

Table 3. The performance of ceramic flaw detection of different algorithms

Algorithm	Input image size	Average accuracy / %	Average recall/ %	Test time/s
Faster R-CNN	640x640	83.18%	84.33%	0.221
Efficientdet-D3	640x640	81.64%	80.18%	0.263
YOLOv5	640x640	87.26%	86.65%	0.192
YOLOX	640x640	90.06%	89.52%	0.181
YOLOv4	640x640	88.35%	89.47%	0.170
Improved Faster R-CNN	640x640	91.72%	92.56%	0.197

4 AI technology-enabled strategies for the development of digital ceramics

Combined with the above analysis of the application of AI technology in digital ceramic technology, the strategy of AI technology to empower the development of digital ceramics is shown in Figure 5, which is based on AI technology, optimizing product design, innovative product manufacturing, and expanding communication channels, etc. and empowers the ceramic industry to keep pace with the times and innovate.

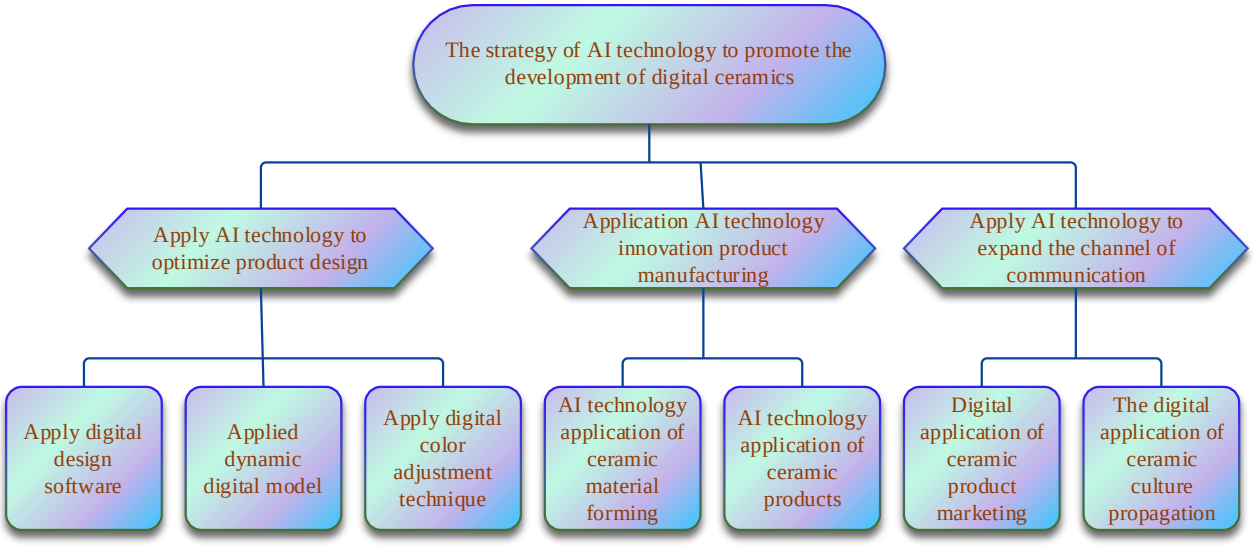

Figure 5. The strategy of AI technology to promote the development of digital ceramics

4.1 Apply AI technology to optimize product design

The first step is to use digital design software. In the digital era, a variety of graphic design and three-dimensional modeling software has emerged, which is applied to the design of ceramic products and has a good application effect.

Second, the application of static and dynamic digital models. Three-dimensional modeling, three-dimensional printing virtual reality, and other technologies used in ceramic product design, such as through the 3D display, a comprehensive three-dimensional presentation of ceramic product design drawings, or with the help of VR glasses and other display equipment, dynamic and static display of ceramic products, for the audit and proofreading to provide a convenient way to modeling, size, pattern, color, and other data to optimize the adjustment.

Lastly, the use of digital color adjustment technology. Based on AI color adjustment technology, specific color digital adjustment can significantly improve the accuracy and richness of the color of ceramic products.

4.2 Applying AI technology to innovative product manufacturing

First, the application of AI technology for molding ceramic materials. Innovative product manufacturing can be achieved through the use of AI technology, particularly digital ceramic molding technology, which is highly creative and practical and better enables the production of complex shapes and structures.

Second, the application of AI technology for firing ceramic products. The application of AI technology can be configured in the firing process of ceramic products, digital automatic control systems, digital functional kilns based on the thixotropic converter, automatic temperature cone, and many other components of the function of the role of the play, greatly enhance the level of intellectualization and the degree of precision, enhance the use of thermal efficiency, shorten the firing time, reduce labor intensity and improve production efficiency.

4.3 Applying AI technology to expand communication channels

The first thing to consider is the digital marketing of ceramic products. AI technical support, through the use of the Internet, digital typesetting three-dimensional display, and other digital technologies, to achieve the digital transformation and reengineering of ceramic products to digital images for exhibition and marketing.

The second aspect is the digital dissemination of ceramic culture. The use of digital technology to integrate and revitalize ceramic culture, promote the digital economy, and deeply integrate the ceramic industry to better enable industrial development. Information technology and VR virtual reality technology can be applied to build a digital museum of ceramic culture, which provides an all-around, three-dimensional display of various types of ceramic products.

5 Conclusion

This study is dedicated to the application of AI technology in ceramics. It proposes to generate digital ceramic texture images by the DCGAN model, detect ceramic defects based on an improved Faster R-CNN algorithm, and analyze the quality of image generation and detection performance. The outcomes are as follows:

1) The images generated by the model in this paper are rated above 4 in terms of image diversity, degree of retention of major texture features, style migration effect, image size, image quality, and the quality of ceramic texture image generation is high. Meanwhile, the ceramic texture image generation of 16384px is realized, the IS score is higher than the comparison algorithm (3.39), and the BRISQUE (22.57) and NIQE (4.43) scores are lower than the other algorithms, which allows the generation of high quality and large size ceramic texture images.

2) The improved Faster R-CNN model in this paper has a detection accuracy of more than 92.68% for stains, foreign objects, multiple golds, damages, and missing ceramics in ceramics. Relative to the original Faster R-CNN algorithm, the detection accuracy and recall have been improved by 8.54% and 8.23%, respectively. The detection time is 0.197s, which provides a better ceramic defect detection performance.

3) The development and application of AI technology have become a strong driving force for industrial upgrading and development. The digital ceramic industry should fully utilize AI technology in the design, production, dissemination, and consumption of ceramic products and actively promote the transformation and upgrading of the ceramic industry development.

References

[1] Liu, K., Hu, J. M., Du, Y. Y., Shi, Y., Sun, Y., & Zhang, S., et al. (2022). Influence of particle size on 3d printed piezoelectric ceramics via digital light processing with furnace sintering. International Journal of Applied Ceramic Technology.

[2] Xia, H., Picart, P., Montresor, & S., et al. (2018). Mechanical behavior of cad/cam occlusal ceramic reconstruction assessed by digital color holography. Dental materials.

[3] Yang, Y., Liu, B., Li, S., Duan, W., & Wang, G. (2023). Non-contact/contact hybrid support based on the slice for ceramic stereolithography. Journal of manufacturing processes.

[4] Wang, S., Peng, L., Song, C., & Wang, C. (2023). Digital light processing additive manufacturing of thin dental porcelain veneers. Journal of the European Ceramic Society.

[5] Chuangang, Y., Weicong, W., Zi, F., & Huade, Z. (2023). Preparation and thermal insulation properties of tpms 3y-tzp ceramics using dlp 3d printing technology. Journal of Materials Science(29), 58.

[6] Bin, S., Mastura, M. I. S., Nazlina, S., Velu, P., Wei, Y., & Leung, M. F. (2022). Innovative collaborative design of ru porcelain shape based on digital shape technology. Mathematical Problems in Engineering, 2022.

[7] Pernot, Jean-Philippe, Veron, Philippe, Danglade, & Florence, et al. (2017). A priori evaluation of simulation models preparation processes using artificial intelligence techniques. Computers in Industry.

[8] Botticelli, M., Mignardi, S., De, V. C., Sala, M., Mazzotta, G., & Da, S. G. L., et al. (2022). The 'metallic ware' from tell el far'ah north (west bank): petrography, technology, and provenance of a hidden ceramic industry. CERAMICS INTERNATIONAL(1), 48.

[9] Doum, J. M., Fuh, G. C., Fadil-Djenabou, S., Onana, V. L., Ndjigui, P. D., & Armstrong-Altrin, J. S. (2020). Characterization and potential application of gleysols and ferralsols for ceramic industry: a case study from dimako (eastern cameroon) (vol 13, 1074, 2020). Arabian journal of geosciences(21), 13.

[10] Ruivo, Luís, Russo, M., Loureno, Rúben, & Pio, D. (2021). Energy management in the portuguese ceramic industry: analysis of real-world factories. Energy, 237.

[11] Yu, G., Ni, Z., Shi, J., Xie, C., Gao, X., & Song, Y. (2022). Shear failure evolution and its dispersion of plain woven ceramic matrix composites z-pin structure. International journal of applied ceramic technology.

[12] Chen, RufeiDuan, WenyanWang, GongLiu, BingshanZhao, YantongLi, Shan. (2021). Preparation of broadband transparent si3n4-sio2 ceramics by digital light processing (dlp) 3d printing technology. Journal of the European Ceramic Society, 41(11).

[13] A, Y. Z., C, P. L. A., B, P. D., A, Y. Z., & A, J. C. (2021). Investigation on 3d printing zro 2 implant abutment and its fatigue performance simulation. Ceramics International, 47(1), 1053-1062.

[14] Tang, D., Yang, K., Gao, T., Liu, T., & Tang, H. (2023). Mechanical-electromagnetic integration design of al_2o_3/sio_2 ceramic cellular materials fabricated by digital light processing. Thin-Walled structures.

[15] Zhang, S., Sutejo, I. A., Kim, J., Yeong-Jin Choi, Park, H., & Hui-suk Yun. (2022). Three-dimensional complex construct fabrication of illite by digital light processing-based additive manufacturing technology. Journal of the American Ceramic Society(6), 105.

[16] Furushima, R., Nakashima, Y., Maruyama, Y., Hirao, K., Ohji, T., & Fukushima, M. (2023). Artificial intelligence-based determination of fracture toughness and bending strength of silicon nitride ceramics. Journal of the American Ceramic Society.

[17] Mu, X. L. H. (2019). Research on ancient ceramic identification by artificial intelligence. CERAMICS INTERNATIONAL, 45(14).

[18] He, Y. (2022). Research on innovative thinking of ceramic art design based on artificial intelligence. Mobile information systems(Pt.2), 2022.

[19] Tian, Y., & Hu, X. (2021). Swot analysis of china's ceramic industry and the use of computers for scientific and technological innovation research. Scientific Programming.